IJITCE

ISSN 2347- 3657

International Journal of Information Technology & Computer Engineering

Email : ijitce.editor@gmail.com or editor@ijitce.com

International Journal of Information Technology & Computer Engineering

ISSN 2347–3657

Volume 8, Issue 3, 2020

Improving Our Knowledge of Driver Qualities by Measuring Their Cognitive Processes

Vidhya B, Suma G C, Dr.Sindhu R

Asst. Prof, Asst. Prof, Asst. Prof

vidhyab.rymec@gmail.com, sumasavita@gmail.com, rethisindhoo@gmail.com

Department of EEE, Proudhadevaraya Institute of Technology, Abheraj Baldota Rd, Indiranagar, Hosapete, Karnataka-583225

Abstract

In this study, we provide a new method for interpreting EEG data collected from drivers during a driving simulator. As indicators of brain nonlinear dynamics, we zeroed in on the Hurst exponent, Shannon entropy, and fractal dimension. While the Hurst exponent shows learning patterns in memory retention and habit development, the Shannon entropy and fractal dimension change during driving condition changes. These trends are statistically significant. These results provide new opportunities for evaluating driver performance, detecting safety hazards, and expanding our knowledge of the non-linear dynamics of human cognition in relation to driving and beyond, and they imply that the tools of Non-linear Dynamical (NLD) Theory can be used as indicators of cognitive state and changes in driving memory. Our research shows that NLD techniques have the ability to shed light on brain states and system variations, which opens the door for their incorporation into existing ML and Deep Learning models. Beyond its use in driving apps, this integration has the potential to enhance cognitive learning, which in turn boosts productivity and accuracy.

Keywords: EEG, Cognition, Fractal Analysis, Hurst Exponent, Shannon Entropy, Fractal Dimension, Non-Linear Dynamics

1. Introduction

Driving is a complex skill that requires many cognitive capabilities. With age and experience, these skills evolve over time. The association between cognitive ability and driving performance is well established [1]. Experience has a significant impact on how cognitive capacities develop, resulting in increases in several areas, such as response time and decision-making ability [2]. Individuals develop a level of familiarity and experience with particular stimuli or tasks via repeated exposure, which results in quicker reaction times [3]. This is frequently seen in activities such as driving, athletics, or video games, where seasoned players react more quickly than inexperienced players. Because the brain may automate some cognitive functions with experience, reaction times shorten as neural pathways become more effective. However, although the experience can enhance cognitive abilities, age-related changes can also have a significant impact on cognitive function [4]. Certain cognitive abilities, such as memory, attention, and executive function, may deteriorate with age [5]. To improve cognitive performance and treat age-related cognitive decline and neurodegenerative illnesses, it is crucial to understand the interaction between experience, aging, and cognitive capacities.

EEG analysis has been used to study driving performance in a variety of ways, including measuring drivers' brain activity while they are taking part in a simulated or real driving test to identify changes in brain activity linked to fatigue, distraction, and other factors that can impair driving performance [6-8]. The study of brain oscillations is another area of EEG analysis in simulated driving [9]. Rhythmic patterns of brain activity in many frequency bands, including the alpha, beta, theta, and gamma bands, are represented by neural oscillations. Decreased alpha oscillations may indicate higher alertness, while increased theta oscillations may indicate cognitive strain or workload [10]. The complexity, regularity, and scaling characteristics of brain activity can also be shown by measurements obtained from EEG data, such as Hurst exponent, Shannon frequency, and fractal dimension. These measurements can be used in the context of simulated driving to evaluate the degree of cognitive engagement, cognitive load, and effectiveness of information processing.

Nonlinear dynamics is a branch of mathematics that studies systems with complicated behaviours that are sensitive to tiny changes in the initial circumstances. It is concerned with the investigation of nonlinear equations and the behaviour of systems, which cannot be simply explained using Newtonian, Hamiltonian, or other linear models. The brain functions as a nonlinear system [11]. This is due to the fact that the brain is made up of billions of neurons that are intricately intertwined. Small changes in the activity of one neuron can have a huge impact on the activity of neighbouring neurons. This can result

in behavioural, perceptual, and cognitive alterations [12]. Nonlinear properties are frequently observed in brain activity data, such as electroencephalography (EEG) or functional magnetic resonance imaging (fMRI) [13]. Linear models may not be sufficient to capture the underlying dynamics or extract meaningful information from such data.

Hurst exponent, a measure of temporal dynamics' "long-term memory," has also been investigated in recent years as a tool for EEG signal interpretation [14]. The Hurst exponent is a mathematical measure used to analyse the long-term memory and predictability of a time series [15]. The Hurst exponent is used in EEG signal analysis to measure the fractal scaling characteristics of the signal, which are connected to the long-range correlations and self-similarities of the time series. By examining the complexity of the EEG signal, the Hurst exponent can be used to distinguish between healthy and pathological brain states [16]. For instance, research has revealed that the Hurst exponents of Alzheimer's patients' EEG signals are lower than those of healthy controls, indicating a loss of complexity and long-range correlations in brain activity [17]. The Hurst exponent has also been found to be altered in various neurological conditions including Parkinson's disease and epilepsy [18,19].

Entropy is a different approach that can be used to extract regular information from EEG datasets [20]. Entropy is a nonlinear property that measures the degree of randomness in a system. Because it cannot be evaluated by frequency relative power derived from linear analysis, it is a useful tool for classifying mental states based on the degree of temporal and spectral irregularity in the EEG signal [21].

The complexity and self-similarity of the EEG data were measured mathematically using the fractal dimension in EEG analysis. It sheds light on the temporal structure and scaling characteristics of the electrical activity of the brain. Fractal dimension is derived from the concept of fractals, which are geometric objects that exhibit self-similarity at different scales. It is calculated by splitting the signal into smaller segments and calculating the fluctuation within each segment. The complexity of the signal increases with fractal dimension.

In EEG analysis, fractal dimension has been used to investigate a number of cognitive processes, such as decision-making, memory, and attention [22]. In addition, they have been used for biomedical signal processing [23,24]. For instance, research has revealed that EEG signals from people with attention deficit hyperactivity disorder (ADHD) have higher fractal dimensions in their EEG signals than those without ADHD [25]. This shows that the increased complexity of brain activity may be linked to ADHD. Additionally, research on brain illnesses, such as Schizophrenia, Depression and Alzheimer's disease, has made use of the fractal dimension [26]. For instance, research has revealed that EEG signals from individuals with Alzheimer's disease are less fractal than those from individuals without Alzheimer's disease [27]. This suggests that Alzheimer's disease may be linked to a decline in cognitive complexity.

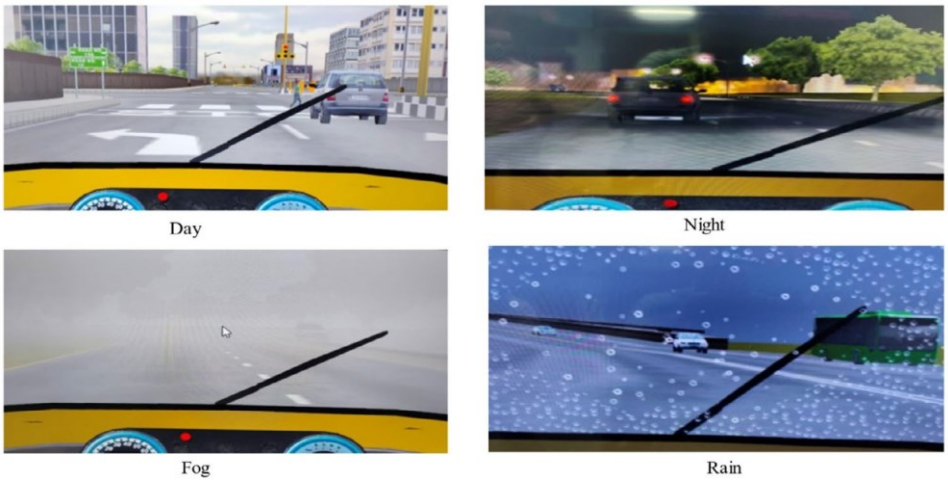

Figure 1: Four Environment Conditions for the Driving Simulator

In this study, we investigated the relationship between age, driving experience, and cognitive processes in driving performance by analysing EEG data collected from drivers and students during a simulated driving test and an on-road experiment. Our approach focused on utilizing nonlinear dynamical parameters to unveil the state of cognition and driving experience embedded in the EEG data. Similar analyses were conducted for EEG & fMRI brain signals solar-cycle activities and also nano-material fabrication [28-30]. Specifically, we computed the Hurst exponent to reveal the retention of memory and experience, while the Fractal Dimension and Shannon Entropy shed light on the complexity of neuronal firing and ease of cognitive processes. By leveraging these nonlinear parameters, we gained insights into the effects of age, driving experience, and task difficulty on driving ability.

2. Materials & Methods

Ten male three-wheeler drivers were selected for this cross-sectional study from five distinct three-wheeler stands (Autorickshaw stands) in Mumbai, India. Participants in the study must possess a valid driving license, have at least two

International Journal of Information Technology & Computer Engineering
ISSN 2347–3657
Volume 8, Issue 3, 2020

years of driving experience, and log at least five hours of driving each day.

The experiment was conducted on drivers in the Ergonomics Laboratory of the National Institute of Industrial Engineering (NITIE), Mumbai, using a fixed three-wheeler driving simulator (Technotrov Systems Pvt. Ltd., Maharashtra, Mumbai; see Fig. 1). This driving simulator is an exact reproduction of a three-wheeled vehicle, complete with all its characteristics. For this experiment, four different traffic situations were selected: low traffic in cities, high traffic in cities, and low traffic on highways. All subjects had 3 min of practice time to become accustomed to the system and procedure, followed

by 15 min of EEG recording.

Figure 2: Photo of a Subject in the 3-Wheeler Driving Simulator with DSI-7 Wireless EEG Headset Mounted on Head

The experiments consisted of four EEG sessions, each lasting approximately four hours, which included four different environments and four traffic conditions for each subject. Thirteen 3-wheeler driver EEG data were collected on the road during high and low traffic conditions for 5 min. Wearable Sensing DSI-7 EEG Headset (Figure 2) was used to collect data from 20 subjects, which is a research-grade EEG sensing device with 8 dry-application sensors, including one for reference (LE) and seven for recording brain wave activity (F3, F4, C3, C4, P3, Pz, P4) [31]. The sampling frequency was set to 300 Hz for the EEG data streamer. The data files that were used for the analyses reported below for all experiments can be found at https://osf.io/8ksyq.

2.1 Data Pre-Processing

EEGLab in MATLAB was used to perform EEG pre-processing using the PREP pipeline [32]. Detrending was carried out to eliminate any cyclical or other patterns and calibrate the thresholds. To eliminate linear trends, a 1 Hz high pass filter was applied [36]. A 50 Hz notch filter was used to eliminate the harsh spectral peaks at 50 Hz. For subsequent processing and feature extraction, the F4 electrode was selected for all individuals based on the spectral decomposition and signal quality.

2.2 Estimation of Hurst Exponent: Nonlinear Dynamical Features

The Hurst Exponent, which depends on the power law [33], was calculated using the Rescaled Range method (R/S) [34].

$$(R/SS)_w \approx kww^H \quad (1)$$

Where, S is the standard deviation of the independent variable x_i within the window w, k is a constant, w is the breadth of the temporal window, and

$$|(tt_0, ww)|^2 \approx \frac{1}{w-1}\sum_{i=t_0}^{t_0+w+1} \approx xx_i - \underline{xx}(tt_0, ww)\approx^2 \quad (2)$$

With average as,

$$\underline{(tt_0, ww)} \approx \frac{1}{w}\sum_{i=t_0}^{t0+w+1} xx_i \quad (3)$$

And R, the range in the time-series, defined as

$$R(tt_0ww) \approx mmaxx \approx_1 mm \approx wwyy(tt_1, ww) - mmmmmm_1 \approx mm \approx wwyy\{tt_0ww\} \quad (4)$$

With the new variables y_i, i=1,2,3,…,w as,

$$yy_i(tt_0, ww) \approx \sum_{k=t_0}^{t0+i+1} \mathbb{k} - x\bar{x}(tt_0, ww)\approx \quad (5)$$

(R/S) was calculated for various time instances, averaged for epochs, and plotted against a log-log axis. The value of H, which ranges from 0 to 1, was determined using the linear regression slope. A time series with a value of H = 0.5 exhibits pure random walking or Brownian motion. On the other hand, H between 0.5 and 1.0 indicates a stable time series. A higher H indicates that the time series has a longer memory and a higher long-term positive autocorrelation or more frequent or persistent deviations. H between 0 and 0.5 indicates anti-persistence, whereas H is more or less equal to 0.5, indicating a random time series [35]. The Hurst exponent was calculated for each of the subjects' 16 sessions over the 10 participants' EEG time series.

International Journal of Information Technology & Computer Engineering
ISSN 2347–3657
Volume 8, Issue 3, 2020

2.3 Estimation of Fractal Dimension

Fractal dimension is a mathematical notion that measures the degree to which a self-similar entity occupies space and is used to measure the complexity of a self-similar object. The box-counting method is a typical method for estimating an object's fractal dimension. It consists of covering the element with a grid of boxes and counting the number of boxes containing a portion of the element. The following is the relationship between the number of boxes N and the box size r:

$$N \sim r^{(-D)} \qquad (6)$$

where the symbol "~" means "proportional to." Taking the logarithm of both sides of the equation yields

$$\log N \sim -D \log r \qquad (7)$$

The slope of the line obtained by plotting log N against log r gives an estimate of the fractal dimension D.

Consider a Koch curve, which is a fractal structure created by constantly adding smaller equilateral triangles to each side of an original triangle. The fractal dimension of the Koch curve was approximately 1.26. The fractal dimension can be estimated using the box-counting approach by covering the curve with a grid of boxes and counting the number of boxes that contain a part of the curve for different box sizes. Using the above equation, the relationship between the number of boxes and the box size can then be used to estimate the fractal dimension.

2.4 Estimation of Shannon Entropy

Because brain activity is a highly dynamic and complicated process involving the interplay of numerous separate neural networks functioning at various frequencies and with differing degrees of synchronization, EEG signals are non-linear, non-stationary, and random. As a result, numerous methods for nonlinear analysis, including entropy, have been proposed to effectively capture the randomness of nonlinear time series data [34].

Let X be a set of finite discrete random variables X= $\{x_1, x_2, x_3, \ldots, x_m\}$, then Shannon entropy, S(X), is defined as:

$$S(X) = -c \sum_{i=0}^{m} (xx_i) \ln pp(xx_i) \qquad (8)$$

Where c is a positive constant acting as a measuring unit and $p(x_i)$ is probability of $x_i \in X$, satisfying:

$$\sum_{i=0}^{m} (xx_i) = 1 \qquad (9)$$

In general, more entropy denotes chaotic or more complex systems, and hence less predictability.

3. Results and Conclusion

The values for H, D & S for all the subjects are summarized in the Table 1 and Pearson Correlation Matrix between all the variables are plotted in Fig 3 below.

Subject	Session	S	H	D	Age		Driving Experience
1	DAY_DRIVING_A	17.62	0.69	1.32	44		24
	DAY_DRIVING_B	17.27	0.73	1.49			
	DAY_DRIVING_C	17.65	0.74	1.43			
	DAY_DRIVING_D	17.72	0.75	1.46			
	FOG_DRIVING_A	16.91	0.78	1.64			
	FOG_DRIVING_B	17.63	0.73	1.55			
	FOG_DRIVING_C	17.16	0.74	1.62			
	FOG_DRIVING_D	17.11	0.77	1.70			
	NIGHT_DRIVING_A	17.30	0.77	1.63			
	NIGHT_DRIVING_B	16.83	0.73	1.48			
	NIGHT_DRIVING_C	17.04	0.78	1.64			
	NIGHT_DRIVING_D	16.80	0.76	1.66			
	RAIN_DRIVING_A	16.97	0.73	1.40			
	RAIN_DRIVING_B	16.79	0.75	1.59			
	RAIN_DRIVING_C	17.09	0.77	1.61			
	RAIN_DRIVING_D	15.91	0.79	1.62			
2	DAY_DRIVING_A	18.02	0.73	1.38	53		17
	DAY_DRIVING_B	17.98	0.75	1.30			
	DAY_DRIVING_C	18.68	0.76	1.47			
	DAY_DRIVING_D	18.59	0.72	1.50			
	FOG_DRIVING_A	18.41	0.72	1.32			
	FOG_DRIVING_B	17.61	0.71	1.55			
	FOG_DRIVING_D	18.94	0.74	1.37			

ISSN 2347–3657
Volume 8, Issue 3, 2020

	NIGHT_DRIVING_A	18.98	0.68	1.43		
	NIGHT_DRIVING_B	15.48	0.68	1.58		
	NIGHT_DRIVING_C	14.61	0.70	1.46		
	NIGHT_DRIVING_D	17.62	0.68	1.61		
	RAIN_DRIVING_A	17.08	0.74	1.39		
	RAIN_DRIVING_B	16.99	0.75	1.44		
	RAIN_DRIVING_C	16.99	0.75	1.44		
	RAIN_DRIVING_D	18.65	0.71	1.40		
3	DAY_DRIVING_A	13.73	0.71	1.26	39	21
	DAY_DRIVING_B	17.35	0.75	1.55		
	DAY_DRIVING_C	17.20	0.73	1.49		
	DAY_DRIVING_D	17.23	0.73	1.50		
	FOG_DRIVING_A	17.66	0.71	1.44		
	FOG_DRIVING_B	17.17	0.73	1.56		
	FOG_DRIVING_C	16.42	0.73	1.33		
	FOG_DRIVING_D	17.37	0.72	1.52		
	NIGHT_DRIVING_A	17.17	0.72	1.36		
	NIGHT_DRIVING_B	17.01	0.76	1.61		
	NIGHT_DRIVING_C	17.20	0.76	1.52		
	NIGHT_DRIVING_D	17.13	0.75	1.50		
	RAIN_DRIVING_A	17.31	0.68	1.46		
	RAIN_DRIVING_B	17.21	0.75	1.49		
	RAIN_DRIVING_C	17.35	0.78	1.49		
	RAIN_DRIVING_D	17.03	0.77	1.55		
4	DAY_DRIVING_A	16.45	0.70	1.25	27	02
	DAY_DRIVING_B	17.66	0.74	1.36		
	DAY_DRIVING_C	17.81	0.72	1.44		
	DAY_DRIVING_D	18.00	0.70	1.29		
	FOG_DRIVING_A	17.86	0.71	1.43		
	FOG_DRIVING_B	17.88	0.67	1.30		
	FOG_DRIVING_C	17.99	0.75	1.52		
	FOG_DRIVING_D	18.37	0.73	1.32		
	NIGHT_DRIVING_A	17.80	0.68	1.35		
	NIGHT_DRIVING_B	17.77	0.68	1.55		
	NIGHT_DRIVING_C	17.98	0.69	1.61		
	NIGHT_DRIVING_D	18.01	0.71	1.26		
	RAIN_DRIVING_A	17.80	0.74	1.47		
	RAIN_DRIVING_B	17.74	0.69	1.63		
	RAIN_DRIVING_C	18.02	0.69	1.33		
	RAIN_DRIVING_D	17.98	0.68	1.48		
5	DAY_DRIVING_A	17.81	0.71	1.41	45	18
	DAY_DRIVING_B	16.36	0.76	1.55		
	DAY_DRIVING_C	17.52	0.70	1.39		
	DAY_DRIVING_D	17.36	0.75	1.56		
	FOG_DRIVING_A	17.99	0.73	1.36		
	FOG_DRIVING_B	17.74	0.73	1.29		
	FOG_DRIVING_C	17.97	0.73	1.36		
	FOG_DRIVING_D	17.83	0.73	1.35		
	NIGHT_DRIVING_A	16.97	0.74	1.30		
	NIGHT_DRIVING_B	17.68	0.74	1.42		

	NIGHT_DRIVING_C	17.69	0.74	1.42		
	NIGHT_DRIVING_D	17.66	0.74	1.36		
	RAIN_DRIVING_A	18.02	0.71	1.43		
	RAIN_DRIVING_B	17.74	0.69	1.34		
	RAIN_DRIVING_C	18.22	0.71	1.45		
	RAIN_DRIVING_D	17.85	0.72	1.32		
6	DAY_DRIVING_A	17.51	0.73	1.38	63	41
	DAY_DRIVING_B	17.50	0.74	1.33		
	DAY_DRIVING_C	17.50	0.72	1.35		
	DAY_DRIVING_D	17.51	0.72	1.32		
	FOG_DRIVING_A	17.63	0.71	1.31		
	FOG_DRIVING_B	17.61	0.71	1.55		
	FOG_DRIVING_C	17.64	0.71	1.43		
	FOG_DRIVING_D	17.72	0.76	1.54		
	NIGHT_DRIVING_A	17.51	0.66	1.37		
	NIGHT_DRIVING_B	17.49	0.72	1.41		
	NIGHT_DRIVING_C	17.51	0.70	1.45		
	NIGHT_DRIVING_D	17.62	0.68	1.61		
	RAIN_DRIVING_A	17.86	0.74	1.39		
	RAIN_DRIVING_B	17.93	0.75	1.40		
	RAIN_DRIVING_C	17.96	0.74	1.41		
	RAIN_DRIVING_D	17.96	0.73	1.36		
7	DAY_DRIVING_A	15.71	0.71	1.50	42	18
	DAY_DRIVING_B	15.71	0.73	1.45		
	DAY_DRIVING_C	15.70	0.75	1.54		
	DAY_DRIVING_D	15.71	0.67	1.32		
	FOG_DRIVING_A	15.71	0.70	1.36		
	FOG_DRIVING_B	15.71	0.73	1.22		
	FOG_DRIVING_C	15.71	0.71	1.38		
	FOG_DRIVING_D	15.71	0.67	1.38		
	NIGHT_DRIVING_A	15.69	0.67	1.55		
	NIGHT_DRIVING_B	15.71	0.71	1.23		
	NIGHT_DRIVING_C	15.71	0.71	1.30		
	NIGHT_DRIVING_D	15.71	0.67	1.34		
	RAIN_DRIVING_A	15.70	0.68	1.45		
	RAIN_DRIVING_B	15.71	0.70	1.46		
	RAIN_DRIVING_C	15.70	0.70	1.49		
	RAIN_DRIVING_D	15.70	0.74	1.49		
8	DAY_DRIVING_A	17.09	0.74	1.39	39	10
	DAY_DRIVING_B	17.85	0.75	1.35		
	DAY_DRIVING_C	18.03	0.70	1.29		
	DAY_DRIVING_D	18.05	0.70	1.31		
	FOG_DRIVING_A	17.01	0.74	1.68		
	FOG_DRIVING_B	17.17	0.75	1.64		
	FOG_DRIVING_C	17.40	0.77	1.42		
	FOG_DRIVING_D	17.52	0.75	1.41		
	NIGHT_DRIVING_A	17.35	0.68	1.53		
	NIGHT_DRIVING_B	16.89	0.68	1.62		
	NIGHT_DRIVING_C	17.12	0.69	1.60		
	NIGHT_DRIVING_D	17.22	0.75	1.64		

	RAIN_DRIVING_A	17.34	0.70	1.35		
	RAIN_DRIVING_B	17.18	0.69	1.36		
	RAIN_DRIVING_C	17.44	0.73	1.47		
	RAIN_DRIVING_D	16.95	0.71	1.61		
9	DAY_DRIVING_A	17.56	0.68	1.53	27	05
	DAY_DRIVING_B	17.65	0.69	1.29		
	DAY_DRIVING_C	17.81	0.72	1.39		
	DAY_DRIVING_D	16.83	0.72	1.50		
	FOG_DRIVING_A	17.82	0.70	1.41		
	FOG_DRIVING_B	17.71	0.72	1.43		
	FOG_DRIVING_C	17.99	0.76	1.51		
	FOG_DRIVING_D	18.01	0.74	1.33		
	NIGHT_DRIVING_A	17.13	0.72	1.40		
	NIGHT_DRIVING_B	17.57	0.71	1.38		
	NIGHT_DRIVING_C	17.63	0.73	1.43		
	NIGHT_DRIVING_D	17.62	0.69	1.31		
	RAIN_DRIVING_A	17.77	0.70	1.46		
	RAIN_DRIVING_B	17.84	0.72	1.31		
	RAIN_DRIVING_C	17.84	0.68	1.32		
	RAIN_DRIVING_D	18.01	0.75	1.36		
10	DAY_DRIVING_A	17.30	0.73	1.35	44	10
	DAY_DRIVING_B	17.48	0.71	1.28		
	DAY_DRIVING_C	17.63	0.69	1.49		
	DAY_DRIVING_D	17.44	0.70	1.33		
	FOG_DRIVING_A	17.23	0.70	1.24		
	FOG_DRIVING_B	17.21	0.72	1.35		
	FOG_DRIVING_C	17.60	0.66	1.38		
	FOG_DRIVING_D	17.61	0.70	1.31		
	NIGHT_DRIVING_A	17.41	0.70	1.30		
	NIGHT_DRIVING_B	17.33	0.70	1.49		
	NIGHT_DRIVING_C	17.35	0.69	1.49		
	NIGHT_DRIVING_D	17.77	0.68	1.31		
	RAIN_DRIVING_A	17.10	0.71	1.42		
	RAIN_DRIVING_B	17.17	0.70	1.38		
	RAIN_DRIVING_C	17.63	0.72	1.55		
	RAIN_DRIVING_D	17.67	0.69	1.56		

Table 1: Tabular data showing the variation in Shannon Entropy (S), Hurst Exponent (H) and Fractal Dimension (D) for the subjects for different sessions and difficulty levels. Sessions were divided into 4 sets comprising of different weather and traffic modes (Highway Low & High Traffic, City Low & High Traffic). Age and Driving Experience of the subjects were also recorded for review.

We conducted an F-Test Two-Sample for Variances to examine the differences in variances between the variables under investigation. The p-values obtained for all pairwise comparisons of variables were found to be less than 0.05 as shown in Table 2, indicating significant differences in variances between the variables.

International Journal of Information Technology & Computer Engineering
ISSN 2347–3657
Volume 8, Issue 3, 2020

	Subject	S		Subject	H		Subject	D
Mean	5.522012579	17.29931	Mean	5.52201258	0.719811	Mean	5.5220126	1.436101
Variance	8.276411114	0.652137	Variance	8.27641111	0.000798	Variance	8.2764111	0.012073
Observations	159	159	Observations	159	159	Observations	159	159
df	158	158	df	158	158	df	158	158
F	12.69121809		F	10370.592		F	685.51322	
P(F<=f) one-tail	5.62503E-47		P(F<=f) one-tail	6.436E-272		P(F<=f) one-tail	8.31E-179	
F Critical one-tail	1.300182044		F Critical one-tail	1.30018204		F Critical one-tail	1.300182	
	Environment	S		Environment	H		Environment	D
Mean	2.503144654	17.29931	Mean	2.50314465	0.719811	Mean	2.5031447	1.436101
Variance	1.264230555	0.652137	Variance	1.26423055	0.000798	Variance	1.2642306	0.012073
Observations	159	159	Observations	159	159	Observations	159	159
df	158	158	df	158	158	df	158	158
F	1.938596991		F	1584.11891		F	104.71287	
P(F<=f) one-tail	1.92043E-05		P(F<=f) one-tail	1.728E-207		P(F<=f) one-tail	6.91E-115	
F Critical one-tail	1.300182044		F Critical one-tail	1.30018204		F Critical one-tail	1.300182	
	Traffic Condition	S		Traffic Condition	H		Traffic Condition	D
Mean	2.496855346	17.29931	Mean	2.49685535	0.719811	Mean	2.4968553	1.436101
Variance	1.264230555	0.652137	Variance	1.26423055	0.000798	Variance	1.2642306	0.012073
Observations	159	159	Observations	159	159	Observations	159	159
df	158	158	df	158	158	df	158	158
F	1.938596991		F	1584.11891		F	104.71287	
P(F<=f) one-tail	1.92043E-05		P(F<=f) one-tail	1.728E-207		P(F<=f) one-tail	6.91E-115	
F Critical one-tail	1.300182044		F Critical one-tail	1.30018204		F Critical one-tail	1.300182	

Table 2: Tabular data showing the F-test Two-Sample for checking the variance between the independent variables (Subject, Simulator Traffic conditions and Environment conditions) and dependent variables (Shannon Entropy (S), Hurst Exponent (H) and Fractal Dimension (D). he p-values obtained for all pairwise comparisons of variables were found to be less than 0.05, indicating significant differences in variances between the variables.

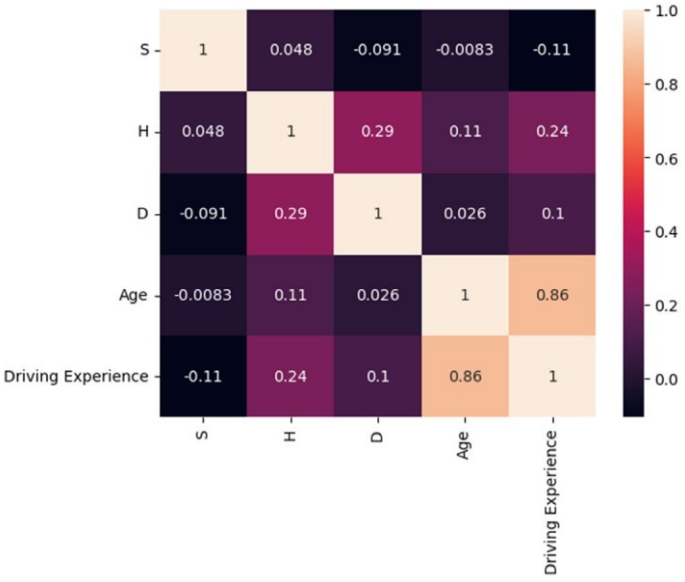

Figure 3: Pearson Correlation Matrix for H, D, S, Driving Experience and Age, Clearly Showing Importance of Incorporating H, D, S While Understanding and Quantifying Driving Experience

International Journal of Information Technology & Computer Engineering
ISSN 2347–3657
Volume 8, Issue 3, 2020

When the difficulty level or weather changed, the driving simulator data analysis showed significant fluctuations in Shannon Entropy (S) and Fractal Dimension (D) as visible in Fig 4 and Fig 5. While D, which denotes complexity or variations in neural patterns, rose during changes in driving circumstances or sessions, S, which stands for chaos and unpredictability, showed considerable swings. Thus, S and D are appropriate markers for investigating sudden changes in driving-related mental states which may be found in the Pearson Correlation Matrix as shown in Fig 3.

Investigations were also conducted on the connection between driving experience and Hurst Exponent (H). H levels varied across driving sessions in subjects of older age and with little prior driving experience as shown in Fig 6. Given that the Hurst Exponent is used to analyze repetitive or memory-related patterns in EEG, the observed fluctuations in H showed weaker retention of driving memory. This research implies that those who have little driving experience and are older may have trouble remembering information about driving over the course of several sessions.

The study also found that H increased when comparing the first and last sessions for each subject, except for those with low driving experience. This suggests that H can serve as a marker for memory retention. Participants with higher H values between the initial and final sessions showed better retention of driving-related information, indicating the role of H in assessing memory retention during driving.

The study findings suggest that S, D, and H can serve as indicators of changes in the mental state and driving memory during driving.

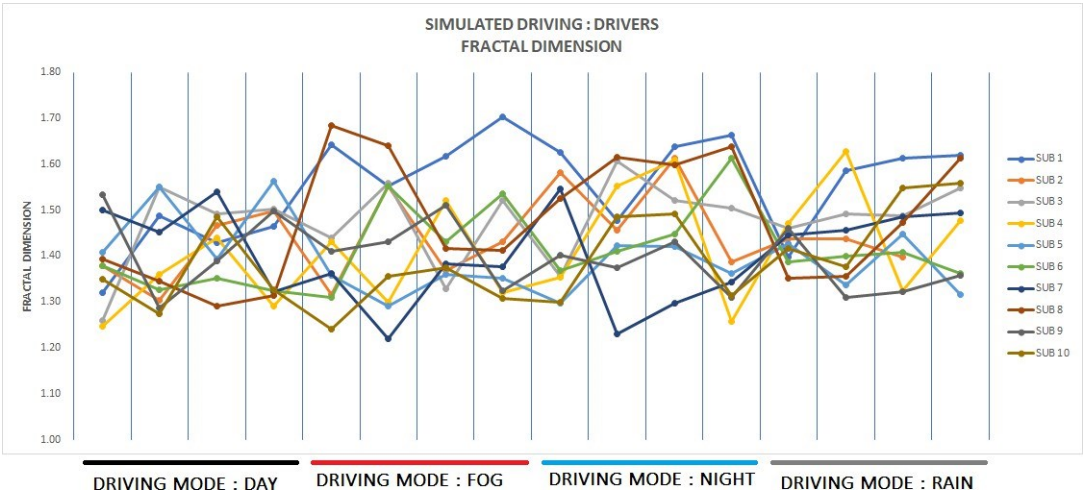

Figure 4: Graph showing the variation of Fractal Dimension in Simulated Driving Experiment for 10 subjects. Each vertical gridline represents the end of an EEG session.

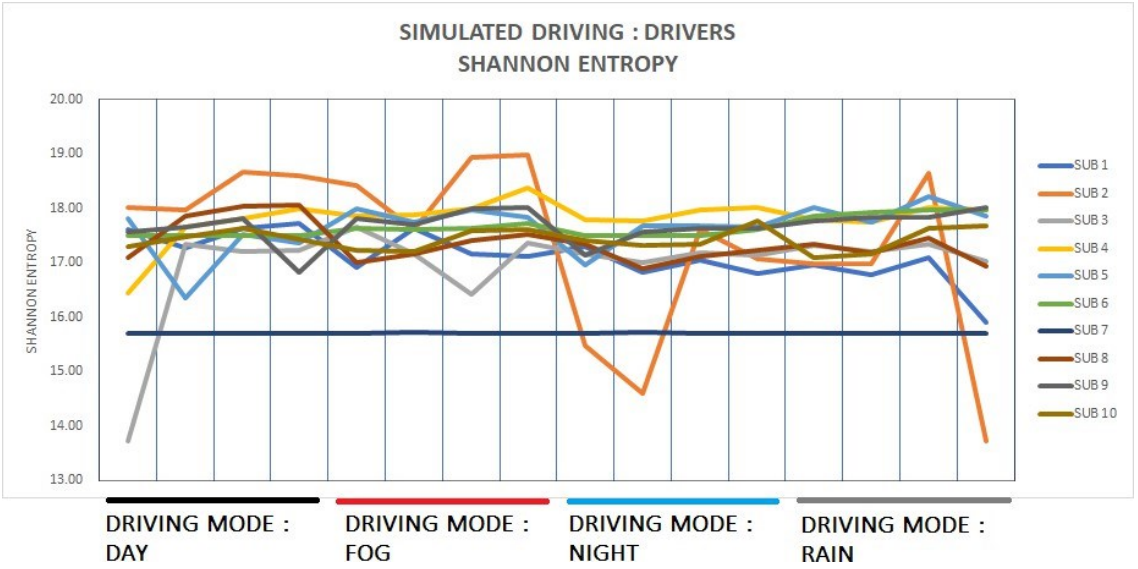

Figure 5: Graph showing the variation of Shannon Entropy in Simulated Driving Experiment for 10 subjects. Each vertical gridline represents the end of an EEG session.

International Journal of Information Technology & Computer Engineering
ISSN 2347–3657
Volume 8, Issue 3, 2020

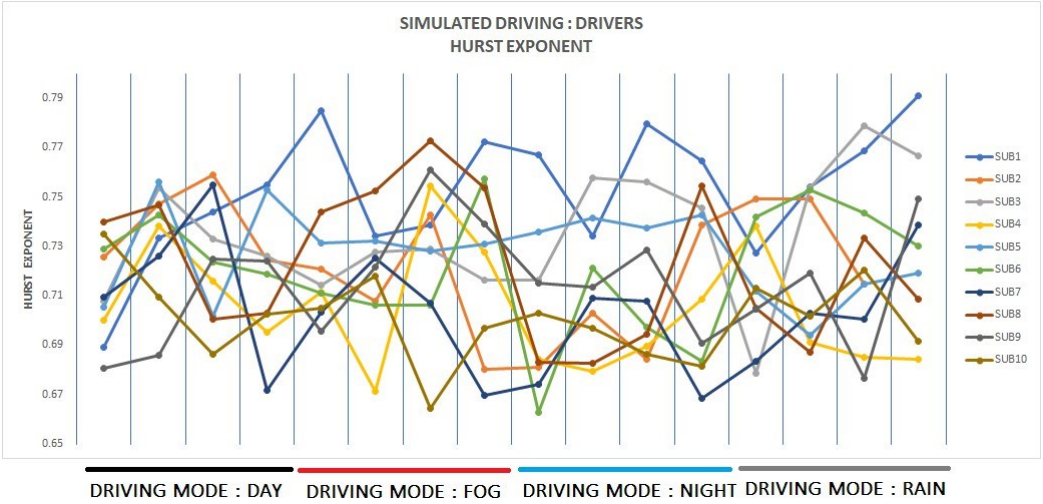

Figure 6: Graph showing the variation of Hurst Exponent in Simulated Driving Experiment for 10 subjects. Each vertical gridline represents the end of an EEG session.

These measures have the potential to develop new approaches for assessing driver performance and identifying safety risks. Moreover, this study demonstrates the applicability of nonlinear dynamical statistics to explain the differences among systems. By applying nonlinear dynamical statistics to the analysis of drivers, this study reveals the relationship between driving experience and age. Therefore, incorporating nonlinear dynamical statistics into existing Deep Learning and Machine Learning models may enhance overall learning and accuracy. Additional research is required to investigate the optimal integration of these markers and validate their efficacy using larger and more diverse datasets derived from cognitive learning experiments.

Credit Authorship Contribution Statement

Pallabjyoti Kakoti: Formal analysis, Software, Visualization, Writing – original draft.

Mukesh Kamti Debnath: Data curation, Investigation, Methodology

Rauf Iqbal: Project administration, Funding acquisition, Resources

Eeshankur Saikia: Conceptualization, Supervision, Writing – review & editing

Acknowledgement

We are thankful towards the autorickshaw drivers of Mumbai, India for giving consent for participating in this study. We also express gratitude towards Ergonomics Lab, NITIE for funding this study.

Conflict of Interest Statement

The authors declare no conflicts of interest.

Data Availability Statement

The EEG data that has been used for the analysis can be found on the following URL: https://osf.io/8ksyq

Compliance with Ethical Standards

All procedures performed in the study involved human participants and all procedures has been carried out in accordance with The Code of Ethics of the World Medical Association (Declaration of Helsinki) for experiments involving humans.

Informed Consent

Informed consent was obtained from all individual participants included in the study.

References

1. De Raedt, R., & Ponjaert-Kristoffersen, I. (2000). The relationship between cognitive/neuropsychological factors and car driving performance in older adults. *Journal of the American Geriatrics Society, 48*(12), 1664-1668.
2. Nabatilan, L. B., Aghazadeh, F., Nimbarte, A. D., Harvey, C. C., & Chowdhury, S. K. (2012). Effect of driving experience on visual behavior and driving performance under different driving conditions. *Cognition, technology & work, 14*, 355-363.
3. Nelson, C. A., Thomas, K. M., & de Haan, M. D. (2012). Neuroscience of cognitive development: The role of experience and the developing brain. John Wiley & Sons.
4. Depestele, S., Ross, V., Verstraelen, S., Brijs, K., Brijs, T., van Dun, K., & Meesen, R. (2020). The impact of cognitive functioning on driving performance of older persons in comparison to younger age groups: A systematic review. *Transportation research part F: trafic psychology and behaviour, 73*, 433-452.
5. Levy, R. (1994). Aging-associated cognitive decline. *International Psychogeriatrics, 6*(1), 63-68.
6. Schier, M. A. (2000). Changes in EEG alpha power during simulated driving: a demonstration. *International Journal of Psychophysiology, 37*(2), 155-162.
7. Karthaus, M., Wascher, E., & Getzmann, S. (2018). Effects of visual and acoustic distraction on driving behavior and EEG in young and older car drivers: a driving simulation study. *Frontiers in aging neuroscience, 10*, 420.
8. Trejo, L. J., Kubitz, K., Rosipal, R., Kochavi, R. L., & Montgomery, L. D. (2015). EEG-based estimation and classification of mental fatigue. *Psychology, 6*(5), 572-589.
9. Lin, C. T., Wu, R. C., Jung, T. P., Liang, S. F., & Huang, T. Y. (2005). Estimating driving performance based on EEG spectrum analysis. *EURASIP Journal on Advances in*

Signal Processing, 2005, 1-10.
10. Teplan, M. (2002). Fundamentals of EEG measurement. *Measurement science review, 2*(2), 1-11.
11. Stam, C. J. (2006). Nonlinear brain dynamics. Nova Publishers.
12. Freeman, W. J., & Vitiello, G. (2006). Nonlinear brain dynamics as macroscopic manifestation of underlying many-body field dynamics. *Physics of life reviews, 3*(2), 93-118.
13. Portnova, G. V., Tetereva, A., Balaev, V., Atanov, M., Skiteva, L., Ushakov, V., & Martynova, O. (2018). Correlation of BOLD signal with linear and nonlinear patterns of EEG in resting state EEG-informed fMRI. *Frontiers in human neuroscience, 11*, 654.
14. Yean, C. W., Khairunizam, W., Omar, M. I., Murugappan, M., Ibrahim, Z., Zheng, B. S., & Mustafa, W. A. (2020). Emotional states analyze from scaling properties of EEG signals using hurst exponent for stroke and normal groups. In *Intelligent Manufacturing and Mechatronics: Proceedings of the 2nd Symposium on Intelligent Manufacturing and Mechatronics–SympoSIMM 2019, 8 July 2019, Melaka, Malaysia* (pp. 526-534). Springer Singapore.
15. Cerqueti, R., & Mattera, R. (2023). Fuzzy clustering of time series with time-varying memory. *International Journal of Approximate Reasoning, 153,* 193-218.
16. Choong, W. Y., Khairunizam, W., Murugappan, M., Omar, M. I., Bong, S. Z., Junoh, A. K., & Mustafa, W. A. W. (2021). Hurst exponent based brain behavior analysis of stroke patients using EEG signals. In *Proceedings of the 11th National Technical Seminar on Unmanned System Technology 2019: NUSYS'19* (pp. 925-933). Springer Singapore.
17. Amezquita-Sanchez, J. P., Mammone, N., Morabito, F. C., Marino, S., & Adeli, H. (2019). A novel methodology for automated differential diagnosis of mild cognitive impairment and the Alzheimer's disease using EEG signals. *Journal of neuroscience methods, 322*, 88-95.
18. Kamalakannan, N., Balamurugan, S. P. S., & Shanmugam, K. (2021). A novel approach for the early detection of Parkinson's disease using EEG signal. *Technology (IJEET), 12*(5), 80-95.
19. Abbasi, M. U., Rashad, A., Basalamah, A., & Tariq, M. (2019). Detection of epilepsy seizures in neo-natal EEG using LSTM architecture. *IEEE access, 7,* 179074-179085.
20. Kannathal, N., Choo, M. L., Acharya, U. R., & Sadasivan, P. K. (2005). Entropies for detection of epilepsy in EEG. *Computer methods and programs in biomedicine, 80*(3), 187-194.
21. Ignaccolo M, Latka M, Jernajczyk W, Grigolini P, West BJ. The dynamics of EEG entropy. *J Biol Phys.* 36:185-196 (2010).
22. John, A. M., Elfanagely, O., Ayala, C. A., Cohen, M., & Prestigiacomo, C. J. (2015). The utility of fractal analysis in clinical neuroscience. *Reviews in the Neurosciences, 26*(6), 633-645.
23. Das, N., Chatterjee, S., Soni, J., Jagtap, J., Pradhan, A., Sengupta, T. K., ... & Ghosh, N. (2013). Probing multifractality in tissue refractive index: prospects for precancer detection. *Optics letters, 38*(2), 211-213.
24. Das, N., Chatterjee, S., Kumar, S., Pradhan, A., Panigrahi, P., Vitkin, I. A., & Ghosh, N. (2014). Tissue multifractality and Born approximation in analysis of light scattering: a novel approach for precancers detection. *Scientific reports, 4*(1), 6129.
25. Dawi, N. M., Kuca, K., Krejcar, O., & Namazi, H. (2021). Complexity and memory-based comparison of the brain activity between ADHD and healthy subjects while playing a serious game. *Fractals, 29*(05), 2150202.
26. Kakoti, P., Syiemlieh, R., & Saikia, E. (2021). New Tool for Detection and Prediction of Major Depressive Disorder. *Advances in Cognitive Psychology, 17*(4).
27. Ahmadlou, M., Adeli, H., & Adeli, A. (2011). Fractality and a wavelet-chaos-methodology for EEG-based diagnosis of Alzheimer disease. *Alzheimer Disease & Associated Disorders, 25*(1), 85-92.
28. Kakoti, P., Syiemlieh, R., & Saikia, E. (2021). Detection, Prediction & Intervention of Attention Deficiency in the Brain Using tDCS. *Machine Learning for Healthcare Applications,* 121-135.
29. Syiemlieh, R., Adhikary, M., Panigrahi, P. K., & Saikia, E. (2022). Analyzing Dominant 13.5 and 27 day Periods of Solar Terrestrial Interaction: A New Insight into Solar Cycle Activities. *Research in Astronomy and Astrophysics, 22*(8), 085005.
30. Saha, R. K., Debanath, M. K., Paul, B., Medhi, S., & Saikia, E. (2020). Antibacterial and nonlinear dynamical analysis of flower and hexagon-shaped ZnO microstructures. *Scientific reports, 10*(1), 2598.
31. Matthews, R., McDonald, N. J., Anumula, H., Woodward, J., Turner, P. J., Steindorf, M. A., ... & Pendleton, J. M. (2007). Novel hybrid bioelectrodes for ambulatory zero-prep EEG measurements using multi-channel wireless EEG system. In *Foundations of Augmented Cognition: Third International Conference, FAC 2007, Held as Part of HCI International 2007, Beijing, China, July 22-27, 2007. Proceedings 3* (pp. 137-146). Springer Berlin Heidelberg.
32. Bigdely-Shamlo, N., Mullen, T., Kothe, C., Su, K. M., & Robbins, K. A. (2015). The PREP pipeline: standardized preprocessing for large-scale EEG analysis. *Frontiers in neuroinformatics, 9*, 16.
33. Suyal, V., Prasad, A., & Singh, H. P. (2009). Nonlinear time series analysis of sunspot data. *Solar Physics, 260*, 441-449.
34. Mandelbrot, B. B., & Wallis, J. R. (1968). Noah, Joseph, and operational hydrology. *Water resources research, 4*(5), 909-918.
35. Phung, D. Q., Tran, D., Ma, W., Nguyen, P., & Pham, T. (2014, April). Using Shannon Entropy as EEG Signal Feature for Fast Person Identification. In *ESANN* (Vol. 4, No. 1, pp. 413-418).
36. Delorme, A., & Makeig, S. (2004). EEGLAB: an open source toolbox for analysis of single-trial EEG dynamics including independent component analysis. *Journal of neuroscience methods, 134*(1), 9-21.